

# Traceable Characterization of THz Electric Fields by Precision Spectroscopy of Cold Trapped HD<sup>+</sup> Ions

Florin Lucian Constantin

Laboratoire PhLAM

CNRS UMR 8523

Villeneuve d'Ascq, France

FL.Constantin@univ-lille1.fr

**Summary**—Terahertz electrometry may be performed by comparing the measurement of the lightshift of a molecular ion transition with the prediction provided by the quantum theory. This contribution proposes to probe the transition  $(v,L)=(0,0) \rightarrow (0,2)$  of cold trapped HD<sup>+</sup> ions in order to characterize a THz electric field slightly detuned to the  $(v,L)=(0,0) \rightarrow (0,1)$  transition of HD<sup>+</sup>. A static magnetic field applied to the ion trap is exploited as a directional reference and to optimize the molecular response to the THz electric field. Weak THz electric fields with amplitudes at the  $\mu\text{V/m}$  level may be detected by performing frequency measurements at the limit of molecular ion quantum projection noise. In addition, the exploitation of six independent lightshift measurements performed for two orientations of the magnetic field enables to characterize conjointly the amplitudes and phases of the Cartesian components of a THz-wave with  $\mu\text{V/m}$ -level and mrad-level uncertainties, respectively.

**Keywords**—two-photon spectroscopy; hydrogen molecular ions; lightshift; Zeeman shift; ab-initio molecular theory; THz sensing

## I. INTRODUCTION

Precision spectroscopy enabled stable and accurate measurements with atoms and molecules and defined the standards for time-frequency and length [1]. During the past decade, the realization of the microwave electric field standard shifted from antennas to Rydberg atom spectroscopy [2]. That enabled SI-traceable measurements, sub-wavelength resolution, accurate, stable and long-term reproducible detection and ensured  $\mu\text{V/cm}$ -level microwave electric field detection with a sensitivity limited by the photon shot noise.

Doppler-free spectroscopy of trapped and sympathetically cooled HD<sup>+</sup> ions in a linear radiofrequency trap allowed recently significant improvements in accuracy and resolution [3-5]. Ab-initio quantum electrodynamics calculations provided accurate predictions for the HD<sup>+</sup> energy levels [6,7] and for their shifts in external fields [8-10]. A double-resonance two-photon spectroscopy scheme may increase the fractional resolution and accuracy with HD<sup>+</sup> ions beyond the  $10^{-12}$  level [11]. The comparison experiment-theory for the lightshifts of a rovibrational transition induced by a THz-wave slightly detuned to the HD<sup>+</sup> energy levels enabled phase-sensitive THz vector electrometry [12]. This contribution discusses the potential of this method using a two-photon rotational transition of HD<sup>+</sup>.

## II. MATERIAL AND METHODS

### A. Double-resonance two-photon spectroscopy of HD<sup>+</sup>

This contribution proposes to exploit the experimental setups used in spectroscopy of trapped and sympathetically cooled HD<sup>+</sup> ions [3-5] for THz electric field sensing. Typically  $\sim 10^2$  HD<sup>+</sup> ions and  $\sim 10^3$  Be<sup>+</sup> ions are maintained in a linear radiofrequency trap. Laser cooling of the Be<sup>+</sup> ions performed at 313 nm enables sympathetical cooling of HD<sup>+</sup>. A static magnetic field is applied to the ion trap with three pairs of coils driven with three independent current sources. The relative orientations of the coil pairs are assumed orthogonal and define the Cartesian laboratory frame (Fig. 1.(a)). The direction of the quantisation axis of the HD<sup>+</sup> ions, defined with the magnetic field, is exploited to relate spectroscopic measurements and parameters of the THz electric field.

The double resonance spectroscopy scheme, shown in Fig. 1.(b), was discussed in ref. [11]. The two-photon rotational transition  $(v,L)=(0,0) \rightarrow (0,2)$  and the two-photon rovibrational transition  $(v,L)=(0,0) \rightarrow (2,0)$  are interrogated conjointly and detected by photodissociating the  $(v,L)=(2,0)$  level with a 175 nm laser. The number of the HD<sup>+</sup> ions in the trap is monitored by exciting their secular motion in the trap and recording the increase of the fluorescence from the laser-cooled Be<sup>+</sup> ions.

The fractional frequency uncertainty of the measurements is estimated with the value of the Allan variance at the molecular ion quantum projection noise limit, expressed as:

$$\sigma_y(\tau) = \frac{1}{\pi Q \sqrt{N_{ion}}} \times \sqrt{\frac{T_c}{\tau}} \quad (1)$$

in function of the quality factor  $Q$  of the two-photon transition, the number  $N_{ion}$  of HD<sup>+</sup> ions, the cycle time  $T_c$ , and the interrogation time  $\tau$ . The quality factor  $Q = f_{2ph}/\Delta f_{HWHM}$ , is expressed in terms of the two-photon frequency and the half-linewidth, estimated using the natural lifetimes of the HD<sup>+</sup> ion energy levels [13]. Assuming the case of single ion spectroscopy experiment with  $T_c = \tau$ , the frequency uncertainty for the  $(v,L)=(0,0) \rightarrow (2,0)$  transition is estimated at 2.49 Hz. For the  $(v,L)=(0,0) \rightarrow (0,2)$  transition, the estimation of the uncertainty is 5.45 mHz, that is by three orders of magnitude better. A significant improvement comparing to the previous

approach [14] is therefore enabled by using the rotational transition.

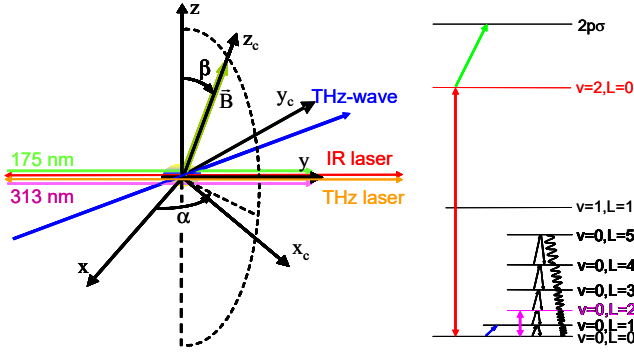


Fig. 1. (a) Experimental setup and coordinate frames : 313 nm cooling laser (magenta line), IR spectroscopy laser (red line), THz spectroscopy laser (orange line), 175 nm dissociating laser (green line). The static magnetic field in the ion trap (olive line) can be oriented to any direction, defined with Euler angles  $(\alpha, \beta)$  in the Cartesian Laboratory Coordinate Frame  $(x, y, z)$  (black lines) (LCF), and THz-wave used in detection (blue line). The standard components of the THz-wave electric field are referenced in the Cartesian Molecular Ion Coordinate Frame  $(x_c, y_c, z_c)$  (black lines) (MICF). (b)  $\text{HD}^+$  spectroscopy scheme: two photon IR and THz transitions (red and magenta lines), dissociation (green line), blackbody radiation driven rotational transitions (black lines), THz-wave electric dipole main coupling (blue line).

A THz electric field is coupled off-resonantly to the rotational transition  $(v, L)=(0, 0) \rightarrow (0, 1)$  at 1.315 THz. The THz electric field is characterized using the measurements of the lightshifts induced on the transitions between the stretched Zeeman sublevels of the  $(v, L)=(0, 0)$  and  $(v, L)=(0, 2)$  states.

### B. *Ab-initio predictions of $\text{HD}^+$ energy levels and shifts in external fields*

The energy levels of  $\text{HD}^+$  are expressed as the sum of the contributions from the rovibrational energy and spin-dependent terms. The rovibrational energy is calculated *ab-initio* by summing the solution of the radial Schrödinger equation and a series expansion of quantum electrodynamics correction terms [6]. The spin structure is due to the coupling of the proton  $\vec{I}_p$ , deuteron  $\vec{I}_d$ , and electron  $\vec{S}_e$  spins with the rotational angular momentum  $\vec{L}$  that yields the total angular momentum  $\vec{J}$ . The eigenvectors  $|vLFSJJ_z\rangle$  are described with the vibrational quantum number denoted  $v$ , the quantum numbers of the squared angular momenta, and of the projection of the total angular momentum on the quantization axis  $J_z$ . The spin energy  $E_{\text{spin}}$  in an external magnetic field is calculated by diagonalizing an effective Hamiltonian for each rovibrational state [7,8].

The shift of a Zeeman level in an external magnetic field of strength  $B$  can be derived approximately from the *ab-initio* calculation using three Zeeman shift  $(t_n, q_n, r_n)$  parameters [8]:

$$\delta E_{n,Z}/h = t_n J_z \cdot B + (q_n + r_n J_z^2) \cdot B^2 \quad (2)$$

The THz electric field in the Cartesian laboratory frame  $\text{LCF}(\vec{e}_x, \vec{e}_y, \vec{e}_z)$  may be expressed as :

$$\vec{E}(t) = \sum_{j=\{x,y,z\}} \frac{E_j \vec{e}_j}{2} \times e^{-i(\omega t + \phi_j)} + c.c. \quad (3)$$

where the components are described with three real positive amplitudes  $E_j$  and two phases  $\phi_x, \phi_y$  (the third is assumed  $\phi_z = 0$ ). The interaction of the THz-wave with the  $\text{HD}^+$  ions may be described using THz electric field standard components in the  $\text{MICF}(\vec{e}_{c,x}, \vec{e}_{c,y}, \vec{e}_{c,z})$  reference frame :

$$\vec{E}(t) = \sum_{q=\{-1,0,1\}} (-1)^q \frac{E_{-q} \vec{e}_q}{2} \times e^{-i(\omega t + \phi_q)} + c.c. \quad (4)$$

with real positive amplitudes  $E_0, E_{\pm 1}$  and phases  $\phi_0, \phi_{\pm 1}$  corresponding to the linear or circular polarizations, defined by  $\vec{e}_0 = \vec{e}_{c,z}, \vec{e}_{\pm 1} = \mp(\vec{e}_{c,x} \pm i\vec{e}_{c,y})/\sqrt{2}$ .

The coupling of the THz electric field to the molecular ions is addressed using the electric dipole approximation. The ac-Stark shift of an energy level is expressed as :

$$\delta E_{n,ac\text{-Stark}} = -\frac{1}{4} \sum_{q=\{-1,0,1\}} (-1)^q |E_{-q}|^2 \alpha_{n,q} \quad (5)$$

in function of the amplitudes  $E_q$  of the standard components of the THz electric field and the standard dynamic polarizabilities  $\alpha_{n,q}$ . The value of the dynamical polarizability and its uncertainty is calculated in function of electric dipole moments, energy levels, and radiative decay rates from refs. [13,15,16], the value of the magnetic field measured by Zeeman spectroscopy, and the frequency of the THz-wave. The fractional uncertainty of the rovibrational energies is assumed at  $10^{-12}$ . Their radiative lifetimes are at the ms level or better. The hyperfine energies are calculated with 0.5 kHz uncertainty. The fractional uncertainty of the Zeeman shift parameters is assumed at  $10^{-4}$  or better. The fractional uncertainty of the electric dipole transition moments is assumed at  $10^{-4}$  or better. The frequency of the THz-wave is assumed known with  $10^{-12}$  fractional uncertainty.

## III. RESULTS

### A. *Characterization of the strength of a magnetic field by Zeeman spectroscopy*

Zeeman spectroscopy of the two-photon rotational transition  $(v, L, F, S, J, J_z) = (0, 0, 1, 2, 2, -2) \rightarrow (0, 2, 1, 2, 4, 0)$  is used here to measure the strength of the static magnetic field applied to the ion trap. The Zeeman shift is calculated approximately with a quadratic dependence:

$$\delta f_Z(B) = \eta_B (\{V_{th}\}) B + \eta_{B^2} (\{V_{th}\}) B^2 \quad (6)$$

in function of the magnetic field strength  $B$ , the linear  $\eta_B$  and quadratic  $\eta_{B^2}$  Zeeman shift coefficients depending on a set of six theoretical parameters  $\{V_{th}\}$  calculated in ref. [8]. The magnetic field strength is derived by inverting eq. (5) and

using the Zeeman shift measured by two-photon rotational spectroscopy and the values for of the theoretical parameters  $\{V_{th}\}$ . Discriminating among two possible solutions can be done by matching the solution for the magnetic field strength value with the result of a supplementary measurement with an accurate magnetometer.

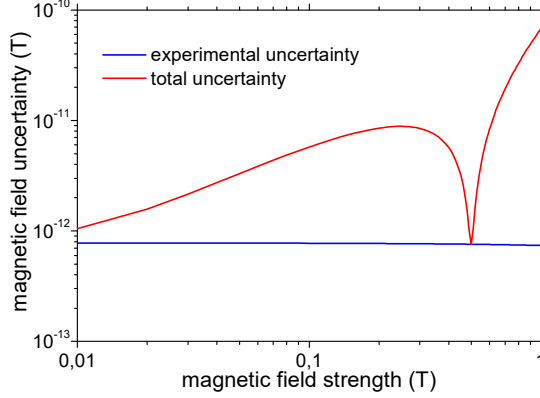


Fig. 2. Uncertainty in the measurement of magnetic field strength by Zeeman spectroscopy of the  $(v,L,F,S,J_z)=(0,0,1,2,2,-2) \rightarrow (0,2,1,2,4,0)$  transition of  $HD^+$ . Total uncertainty of the magnetic field (red line) and contribution from the frequency measurement uncertainty (blue line).

The uncertainty of the magnetic field strength is derived by propagating the errors from the Zeeman shift frequency measurement  $u(\delta f_z) = 5.45 \cdot \sqrt{2} \text{ mHz}$  and from the Zeeman shift parameters  $u(q_{1,2}) = u(r_{1,2}) = 50 \text{ MHz/T}^2$ ,  $u(t_{1,2}) = 5 \text{ kHz/T}$ .

The uncertainty of the magnetic field derived by Zeeman spectroscopy in function of the magnetic field strength is shown in Fig. 2, as well as the partial contribution from experimental uncertainties. The accuracy of the calibration of the magnetic field by spectroscopy, in the range of  $10^{-12} \text{ T}$  to  $10^{-10} \text{ T}$ , is limited by the theory errors in this range of magnetic field strengths. The contribution from the experimental errors is below the  $10^{-12} \text{ T}$  level.

#### B. Determination of the amplitude of a THz electric field: sensitivity and accuracy issues

For a  $\pi$  or  $\sigma^\pm$ -polarized THz electric fields derived from a lightshift measurement, the uncertainty is evaluated by translating the uncertainties from the frequency measurements and from the *ab-initio* calculations of the theoretical parameters. For example, the measurement of the lightshift of the  $(v,L,F,S,J_z)=(0,0,1,2,2,2) \rightarrow (0,2,1,2,4,4)$  transition may allow detection of a  $\sigma$ -polarized THz-wave at 1,314,947,502.3 kHz with an amplitude as low as  $7 \text{ } \mu\text{V/m}$  by optimizing the strength of the magnetic field in the ion trap. That improves the sensitivity of the THz electric field detection nearly thirty times comparing to the microwave electrometry result based on the Rydberg atom spectroscopy method [2].

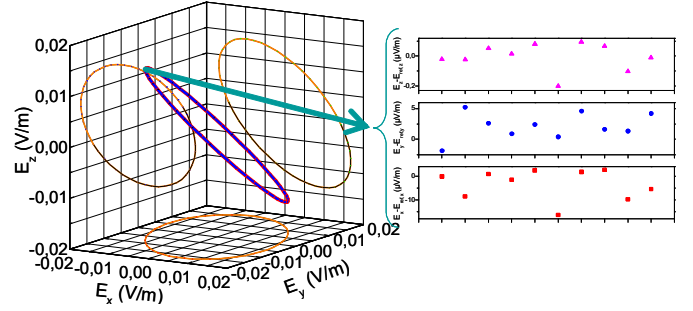
The precision of the calibration of the THz-wave intensity using lightshift measurements is estimated also by minimizing the uncertainty using an optimized value of the magnetic field

in the trap. A fractional uncertainty of  $10^{-3}$  in THz-wave intensity calibration may be reached for a THz-wave with  $10 \text{ mW/m}^2$  intensity. This estimation is limited by the accuracy of the dynamic polarizability calculation.

#### C. Three-dimensional characterization of a THz-wave using $HD^+$ spectroscopy

The polarization ellipse (PE) of a THz electric field in three dimensions, described in the laboratory frame with three real positive amplitudes and two phases  $(E_x, E_y, E_z, \phi_x, \phi_y)$ , may be fully characterized using lightshift measurements. Let's consider a  $\sigma^+$ -polarized reference THz-wave at 1,314,947,502.3 kHz with an intensity of  $1 \text{ W/m}^2$  propagating along a direction defined with Euler angles  $(\alpha, \beta) = (\pi/4, \pi/4)$  in the laboratory frame. The PE of this THz-wave may be determined from a set of six independent lightshift measurements of  $(v,L,F,S,J_z) = (0,0,1,2,2,2) \rightarrow (0,2,1,2,4,4)$  for three magnetic fields  $B_1 = 1 \text{ } \mu\text{T}$ ,  $B_2 = 5 \text{ } \mu\text{T}$ ,  $B_3 = 10 \text{ } \mu\text{T}$  and two orientations defined with the Euler angles  $(\alpha, \beta) = (0,0)$  and  $(\alpha, \beta) = (0, \pi/2)$ .

Fig. 3. Polarization ellipse (PE) for the reference THz-wave (red curve) and PE retrieved from lightshift measurements (blue curves). Inset: deviations of the measured electric field amplitudes from the corresponding amplitudes of the reference THz-wave.



The experimental lightshifts are simulated by adding to the theoretical values random frequency shifts with a Gaussian distribution with zero mean and standard deviation given by the lightshift measurement uncertainty. The dynamic polarizabilities are evaluated as the theoretical value plus a random contribution with a Gaussian distribution with zero mean and standard deviation given by the dynamic polarizability calculation uncertainty. That enables to derive the squared standard components of the THz electric field relative to both orientations of the quantization axis. Then, the parameters of the THz electric field in the laboratory frame are calculated analytically. The retrieved PE of the THz-wave from 10 sets of lightshift measurements are represented in Fig. 3. The uncertainties of the amplitudes and phases of the Cartesian components of the THz electric field in the laboratory frame are at the  $(\delta E_x = \delta E_y = 1 \text{ } \mu\text{V/m}, \delta E_z = 0.1 \text{ } \mu\text{V/m}, \delta \phi_x = 1 \text{ mrad}, \delta \phi_y = 1 \text{ mrad})$  levels. The inset of Fig. 3 indicates the shifts of the amplitudes of the Cartesian components of the retrieved electric fields from the values of the reference THz-wave.

#### IV. CONCLUSIONS

This contribution proposes a new approach to characterize a THz-wave by comparing the measurements of the frequency shifts of  $\text{HD}^+$  transitions with the predictions of the molecular ion theory. That enables a direct link of the THz electric fields to the SI second and to the fundamental constants. This method enables weak THz electric field sensing at the  $\mu\text{V/m}$  level and retrieval of the amplitudes and phases of the Cartesian components of a THz electric field with  $\mu\text{V/m}$  and mrad accuracies, respectively, that are significant improvements beyond the state-of-the-art electrometry performed by Rydberg state spectroscopy of alkali vapours.

#### REFERENCES

- [1] F. Riehle *et al.*, “The CIPM list of recommended frequency standard values: guidelines and procedures,” *Metrologia*, vol. 55, pp. 188–200, February 2018.
- [2] C.S. Adams, J.D. Pritchard, and J.P. Shaffer, “Rydberg atom quantum technologies,” *J. Phys. B*, vol. 53, pp. 012002, December 2020.
- [3] S. Alighanbari *et al.*, “Precise test of quantum electrodynamics and determination of fundamental constants with  $\text{HD}^+$  ions,” *Nature*, vol. 581, pp. 152–158, May 2020.
- [4] S. Patra *et al.*, “Proton-electron mass ratio from laser spectroscopy of  $\text{HD}^+$  at the part-per-trillion level,” *Science*, vol. 369, pp. 1238–1241, July 2020.
- [5] I.V. Kortunov *et al.*, “Proton-electron mass ratio by high-resolution optical spectroscopy of ion ensembles in the resolved-carrier regime,” *Nat. Phys.*, vol. 17, pp. 569–573, February 2021.
- [6] V.I. Korobov, L. Hilico, and J.-P. Karr, “Fundamental transitions and ionization energies of the hydrogen molecular ions with few ppt uncertainty,” *Phys. Rev. Lett.*, vol. 118, pp. 233001, June 2017.
- [7] D. Bakalov, V.I. Korobov, and S. Schiller, “High-precision calculation of the hyperfine structure of the  $\text{HD}^+$  ion,” *Phys. Rev. Lett.*, vol. 97, pp. 243001, December 2006.
- [8] D. Bakalov, V.I. Korobov, and S. Schiller, “Magnetic field effects in the transitions of the  $\text{HD}^+$  molecular ion and precision spectroscopy,” *J. Phys. B*, vol. 44, pp. 025003, January 2011.
- [9] S. Schiller *et al.*, “Static and dynamic polarizability and the Stark and blackbody-radiation frequency shifts of the molecular hydrogen ions  $\text{H}_2^+$ ,  $\text{HD}^+$ , and  $\text{D}_2^+$ ,” *Phys. Rev. A*, vol. 89, pp. 052521, May 2014.
- [10] D. Bakalov and S. Schiller, “The electric quadrupole moment of molecular hydrogen ions and their potential for a molecular ion clock,” *Appl. Phys. B*, vol. 114, pp. 213–230, January 2014.
- [11] F.L. Constantin, “Double-resonance two-photon spectroscopy of hydrogen molecular ions for improved determination of fundamental constants,” *IEEE Trans. Instrum. Meas.*, vol. 68, pp. 2151–2159, March 2019.
- [12] F.L. Constantin, “Phase-sensitive vector terahertz electrometry from precision spectroscopy of molecular ions,” *Atoms*, vol. 8, pp. 70, October 2020.
- [13] Z. Amitay, D. Zajfman, and P. Forck, “Rotational and vibrational lifetime of isotopically asymmetrized homonuclear diatomic molecular ions,” *Phys. Rev. A*, vol. 50, pp. 2304–2308, September 1994.
- [14] F.L. Constantin, “Sensing a THz electric field with a molecular ion clock,” *Proceedings of the SPIE*, vol. 11700, pp. 1170046, March 2021.
- [15] R.E. Moss, “Calculations for vibration-rotation levels of  $\text{HD}^+$ , in particular for high  $N$ ,” *Mol. Phys.*, vol. 78, pp. 371–405, March 1993.
- [16] Bakalov, D. and Schiller, S., “Static Stark effect in the molecular ion  $\text{HD}^+$ ,” *Hyperfine Interact.*, vol. 210, pp. 25–31 January 2012.